AGU PUBLICATIONS

Earth and Space Science

Supporting Information for

The Mass Change Designated Observable Study: Overview and Results

D. N. Wiese[1], B. Bienstock[1], C. Blackwood[1], J. Chrone[2], B. D. Loomis[3], J. Sauber[3], M. Rodell[3], R. Baize[2], D. Bearden[1], K. Case[1], S. Horner[4], S. Luthcke[3], J. T. Reager[1], M. Srinivasan[1], L. Tsaoussi[5], F. Webb[1], A. Whitehurst[5], V. Zlotnicki[1]

[1]Jet Propulsion Laboratory, California Institute of Technology

[2]NASA Langley Research Center

[3]NASA Goddard Space Flight Center

[4]NASA Ames Research Center

[5]NASA Headquarters

Contents of this file

Introduction

The supplementary information provides additional information regarding architecture and technology definition, numerical simulation setup, and supporting figures for the main analysis in the paper.

Text S1.

The architecture trade space is essentially infinite given the multiple variables that impact the science value of the architectures listed in Table S2. The set of simulated architectures was selected such that the boundary conditions were explored to capture the full range of possible outcomes. For example, it is undesirable to fly at an altitude above 500 km due to the attenuation of gravity signals with increasing altitude; 350 km is an approximate lower limit given the increased drag forces that exist at lower altitudes. The selected separation distance is far less of a factor than the altitude but does affect the measurement system value to an extent that it must be considered. Results presented in Section 6 consistently use a 300 km separation distance, as simulations showed this to be the preferred value. Note this separation distance is slightly larger than the nominal operational separation distance of GRACE and GRACE-FO (220 +/- 50 km), as we find the impact of accelerometer error on the gravity retrieval is lessened with larger separation distances. The selected pendulum opening angles are informed by the results of Li et al. (2016). AIGG simulations were performed for a single instrument oriented in the radial, along-track, and cross-track directions, with the radial configuration performing approximately an order of magnitude better than the other orientations; thus, the results presented here focus on the radial orientation. We assumed three AIGG beams with a 2-meter baseline and 15 second interrogation time, resulting in a sensitivity of 10^{-5} Eötvös and a sample rate of 0.1 Hz. Table S2 provides a summary of the simulated architectures, while Tables S3 and S4 provide summaries of the inter-satellite ranging technologies and accelerometer technologies. The technologies in Tables S3 and S4 were appropriately mixed and matched across the architectures described in Table S2 to provide a large trade space of potential architecture variants (see Figure 1). The performance metrics in Table S2 and S3 are approximations of performance based on a specific frequency band; in reality, a full error spectra across relevant frequency bands is taken into account in the numerical simulations.

Text S2.

Force models used in the numerical simulations to derive science value are given in Table S5. To derive measurement system value (i.e., neglecting temporal aliasing error), the nominal models in Table S5 are set equivalent to the truth models. All models are expressed to spherical harmonic degree and order 180. Additional conservative force models considered in the numerical simulations include third body effects (DE421b), General Relativistic Effects (IERS2010), S1 and S2 air tides (Ray and Ponte, 2003), and Solid Earth and Ocean Pole Tides (IERS2010). Non-gravitational forces considered in the simulations include atmospheric drag, solar radiation pressure, and Earth radiation pressure.

Gravity fields are estimated to spherical harmonic degree and order 180 covering the span January 1-29, 2006. Gravity estimation is a 2-step process, where in the first step, a set of "local" parameters are estimated using the tracking data for the purposes of converging the orbit. The estimated parameters in the first step include daily position and velocity of each spacecraft, daily accelerometer scale factors, daily accelerometer biases, and a range-rate bias, range-rate drift, and a range-rate one cycle per revolution. In the second step of the gravity estimation, these same parameters are estimated again along with the 29-day mean gravity field expressed to spherical harmonic degree and order 180. Additionally, a covariance function for each data type and relative weights for each day are estimated in an iterative manner (second step only) as described in Ellmer (2018).

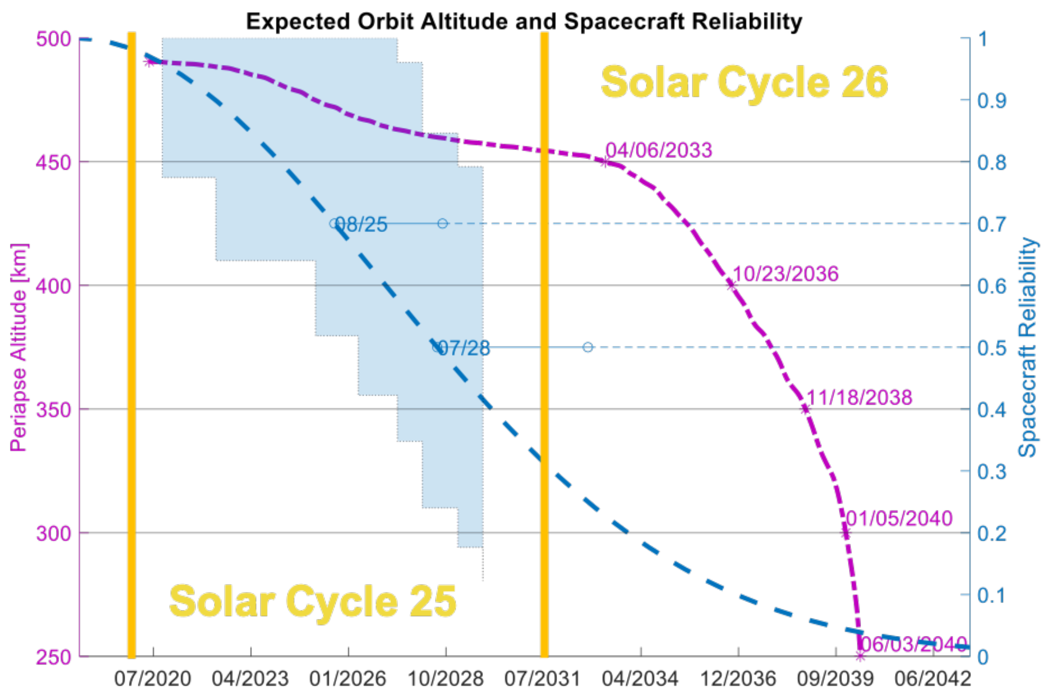

Figure S1. Triggering mechanisms for GRACE-FO end of life, showing spacecraft reliability estimates (y-axis, right) in the dashed blue line with 2-sigma uncertainty estimates in shaded blue, and orbital altitude degradation due to increasing atmospheric drag forces (y-axis, left). Altitude degradation is computed using the 2-sigma (95% confidence) Schatten solar cycle predictions from the Goddard Flight Dynamics Facility. We note solar cycle predictions are inherently uncertain; stronger solar cycles than simulated here will lead to more rapid altitude degradation.

Decadal Survey Science Topics, Questions, Objectives, and Geophysical Observables						Mapping to MC Observables (Community Interpretation)			
Topic	**DS Science Question**	**DS Science/Application Objective**	**Necessary observables**	**Current state of the art for Science/Application Obective**	**Importance of Objective specificed in DS**	**Utility. Relative importance of Mass Change to achieve DS Science/Appobjective**	**DS Suggested Measurement Parameters for MC Baseline. Most imporant variable is in bold**	**DS Suggested Measurement Parameters for MC Goal. Most important variable is in bold**	**Justification for Suggested Measurement Parameters: Both Baseline and Goal**
Climate Variability and Change	***C-1.*** How much will sea level rise, globally and regionally, over the next decade and beyond, and what will be the role of ice sheets and ocean heat storage?	C-1a. Determine the global mean sea level rise to within 0.5 mm yr-1 over the course of a decade	Sea Surface Height Terrestrial Reference Frame Ocean Mass Redistribution	precision: +/-0.5mm yr-1 (0.4 mm yr-1 from altimetry, 0.3 mm yr-1 from ocean mass [Watkins et al., 2015])	Most Important	High. MC provides a unique measurement of global ocean mass change.	Ocean Mass distribution **Spatial Resolution: (300 km)^2** Temporal Resolution: monthly Accuracy: 15 mm	Ocean Mass distribution **Spatial Resolution: (100 km)^2** Temporal Resolution: monthly Accuracy: 15 mm	**Baseline:** Specified in the Decadal Survey (Appendix B) **Goal:** Higher spatial resolution will reduce land leakage errors which are one of the dominant sources of error in determining global ocean mass.
		C-1b. Determine the change in the global oceanic heat uptake to within 0.1 Wm-2 over the course of a decade	Sea Surface Height Ocean Mass Redistribution Ocean Temperature and Salinity Profile	precision: +/-0.44 W m-2 over 10 ys (same as C-1a)	Most Important	High. Ocean heat uptake is related to total sea surface height minus ocean mass component. This serves as an independent measurement of planetary heat uptake.	Ocean Mass distribution **Spatial Resolution: (300 km)^2** Temporal Resolution: monthly Accuracy: 15 mm	Ocean Mass distribution **Spatial Resolution: (100 km)^2** Temporal Resolution: weekly Accuracy: 15 mm	**Baseline:** Specified in the Decadal Survey (Appendix B) **Goal:** Higher spatial resolution will reduce land leakage errors which are one of the dominant sources of error in determining global ocean mass.
		C-1c. Determine the changes in total ice sheet mass balance to within 15 Gton/yr over the course of a decade and the changes in surface mass balance and glacier ice discharge with the same accuracy over the entire ice sheets, continuously, for decades to come	Ice sheet mass change Ice sheet velocity Ice sheet elevation Ice sheet thickness Ice shelf thickness Ice sheet bed elevation Ice shelf cavity shape Ice sheet surface mass balance	precision: +/-24 Gt yr-1 (Greenland), +/-39 Gt yr-1 (Antarctica) [Watkins et al., 2015]	Most Important	High. Ice sheet mass change is directly and uniquely measured through MC.	Ice Sheet Mass distribution **Spatial Resolution: (300 km)^2** Temporal Resolution: monthly Accuracy: 40 mm	Ice Sheet Mass distribution **Spatial Resolution: (100 km)^2** Temporal Resolution: monthly Accuracy: 10 mm	**Baseline:** Consistency with the current program of record **Goal:** Specified in the Decadal Survey (Appendix B)
		C-1d. Determine regional sea level change to within 1.5- 2.5 mm/yr over the course of a decade (1.5 corresponds to a ~(6000 km)^2 region, 2.5 corresponds to a ~(4000 km)^2 region)	Sea surface height Vertical Land motion Ocean mass distribution Wind Vector	signals: <5 mm yr-1 signal, ocean mass trends [Watkins et al., 2015]; <2.5 mm yr-1 signal, sea level fingerprints	Very important	High. MC provides a unique measurement of ocean mass change.	Ocean Mass distribution **Spatial Resolution: (300 km)^2** Temporal Resolution: monthly Accuracy: 15 mm	Ocean Mass distribution **Spatial Resolution: (100 km)^2** Temporal Resolution: monthly Accuracy: 15 mm	**Baseline:** Specified in the Decadal Survey (Appendix B) **Goal:** Higher spatial resolution will reduce land leakage errors which are one of the dominant sources of error in determining regional ocean mass.
	C-7. How are decadal scale global atmospheric and ocean circulation patterns changing, and what are the effects of these changes on seasonal climate processes, extreme events, and longer term environmental change?	C-7d. Quantify the linkage between the dynamical and thermodynamic state of the ocean upon atmospheric weather patterns on decadal timescales. Reduce the uncertainty by a factor of 2 (relative to decadal prediction uncertainty in IPCC 2013). Confidence level: 67% (likely).	Ocean velocity Ocean temerature Ocean salinity Wind Stress Ocean bottom pressure/ocean mass Many other pertinent variables	Ocean bottom pressure measurements contribute to the understanding of dynamic changes of the ocean on monthly to decadal timescales (e.g., Johnson and Chambers, 2013). When combined with SSH, ocean mass contributes to the understanding of the thermodynamic state.	Important	Low. MC is a secondary observable for this objective.	Ocean Mass distribution **Spatial Resolution: (300 km)^2** Temporal Resolution: monthly Accuracy: 15 mm	Ocean Mass distribution **Spatial Resolution: (50 km)^2** Temporal Resolution: monthly Accuracy: 10 mm	**Baseline:** Consistency with the current program of record **Goal:** Specified in the Decadaly Survey (Appendix B). Higher spatial resolution will allow for resolution of major oceanic fronts.
		C-7e. Observational verification of models used for climate projections. Are the models simulating the observed evolution of the large scale patterns in the atmosphere and ocean circulation, such as the frequency and magnitude of ENSO events, strength of AMOC, and the poleward expansion of the sub-tropical jet (to a 67% level correspondence with the observational data)?	Ocean velocity Ocean temerature Ocean salinity Wind Stress Ocean bottom pressure/ocean mass Many other pertinent variables	Similar to C-7d. Indication for signatures of the AMOC can be found in ocean bottom pressure data (e.g., Landerer et al., 2015)	Important	Low. MC is a secondary observable for this objective.	Ocean Mass distribution **Spatial Resolution: (300 km)^2** Temporal Resolution: monthly Accuracy: 15 mm	Ocean Mass distribution **Spatial Resolution: (50 km)^2** Temporal Resolution: monthly Accuracy: 10 mm	**Baseline:** Consistency with the current program of record **Goal:** Specified in the Decadaly Survey (Appendix B). Higher spatial resolution will allow for resolution of major oceanic fronts.
Global Hydrological Cycles and Water Resources	**H-1.** How is the water cycle changing? Are changes in evapotranspiration and precipitation accelerating, with greater rates of evapotranspiration and thereby precipitation, and how are these changes expressed in the space-time distribution of rainfall, snowfall, evapotranspiration, and the frequency and magnitude of extremes such as droughts and floods?	H-1a. Develop and evaluate an integrated Earth System analysis with sufficient observational input to accurately quantify the components of the water and energy cycles and their interactions, and to close the water balance from headwater catchments to continental-scale river basins.	Precipitation (GPM; A-CCP), Evapotranspiration (thermal imagers) Runoff (SWOT), Terrestrial water storage mass change (dTWS) (MC).	Water budget closure at continental, monthly and annual scales with less than 10% (of precipitation total) uncertainty [Rodell et al., 2015]	Most Important	High: dTWS is essential to closing the water budget, i.e., dTWS = P - ET - Q, and only a mass change measurement can provide it.	Terrestrial Water Storage Mass Change Spatial Resolution: (1,000 km)^2 Temporal Resolution: monthly **Accuracy: 10 mm**	Terrestrial Water Storage Mass Change Spatial Resolution: (3 km)^2 Temporal Resolution: monthly **Accuracy: 10 mm**	**Baseline:** Consistency with the current program of record, allowing water budget closure at continental, monthly and annual scales with less than 10% (of precipitation) total uncertainty. **Goal:** Improved spatial resolution enabling water budget closure at the scale of headwater catchments.
	H-2. How do anthropogenic changes in climate, land use, water use, and water storage interact and modify the water and energy cycles locally, regionally and globally and what are the short and long-term consequences?	H-2c. Quantify how changes in land use, land cover, and water use related to agricultural activities, food production, and forest management affect water quality and especially groundwater recharge, threatening sustainability of future water supplies.	dTWS (MC) and either (1) simplifying assumptions; or (2) precipitation (GPM; A-CCP), solar radiation (multiple), soil moisture (SMAP, SMOS), land cover and irrigation information (imagers), and a hydrological model	In certain arid regions and regions with sufficient auxiliary hydrological information, groundwater recharge can be estimated from GRACE and GRACE-FO dTWS at the scales of those missions [Henry et al., 2011; Gonçalvès et al., 2013; Mohamed et al., 2017]	Most Important	High: dTWS can be used to infer dGW (with auxiliary info or assumptions), which is essential to estimating GW recharge as the sum of dGW and GW discharge, however, estimates of the latter variable are also needed.	Terrestrial Water Storage Mass Change **Spatial Resolution: (450 km)^2** Temporal Resolution: monthly Accuracy: 25 mm	Terrestrial Water Storage Mass Change **Spatial Resolution: (50 km)^2** Temporal Resolution: monthly Accuracy: 10 mm	**Baseline:** Consistency with the current program of record, which has supported estimates of dGW at regional scales. **Goal:** Specified in the Decadal Survey (Table 6.3: "basin scale (50 km or better)").
	H-3. How do changes in the water cycle impact local and regional freshwater availability, alter the biotic life of streams, and affect ecosystems and the services these provide?	H-3b. Monitor and understand the coupled natural and anthropogenic processes that change water quality, fluxes, and storages in and between all reservoirs (atmosphere, rivers, lakes, groundwater, and glaciers), and response to extreme events.	Numerous terrestrial water cycle observations including dTWS (MC).	dTWS observed by GRACE with 1-2 cm uncertainty over monthly and >(450 km)^2 scales [other analysis (accounting for leakage) reports 1 cm at (1000 km)^2] [Landerer et al., 2020]	Important	High: Monitoring and understanding dTWS provides clues to the natural and anthropogenic processes that control water storage changes and	Terrestrial Water Storage Mass Change **Spatial Resolution: (450 km)^2** Temporal Resolution: monthly Accuracy: 25 mm	Terrestrial Water Storage Mass Change **Spatial Resolution: (200 km)^2** Temporal Resolution: monthly Accuracy: 25 mm	**Baseline:** Consistency with the current program of record, which has supported estimates of dTWS at regional scales. **Goal:** Improved spatial resolution would allow for quantification of dTWS at scales that better support process understanding.
	H-4. How does the water cycle interact with other Earth System processes to change the predictability and impacts of hazardous events and hazard-chains (e.g. floods, wildfires, landslides, coastal loss, subsidence, droughts, human health, and ecosystem health), and how do we improve preparedness and mitigation of water-related extreme events?	H-4c. Improve drought monitoring to forecast short-term impacts more accurately and to assess potential mitigations.	Precipitation (GPM, A-CCP), soil moisture (SMAP, SMOS), dTWS (MC), surface waters (SWOT), vegetation health and evapotranspiration (imagers).	Drought/wetness monitoring via GRACE-based indices (monthly and >(450 km)^2 scales) [Thomas et al., 2014; Zhao et al., 2017] or via GRACE data assimilation (weekly and (12 km)^2 scales) [Houborg et al., 2012; Li et al., 2019]; accuracy not quantified.	Important	Medium: Satellite gravimetry based observations of TWS anomalies are useful indicators of drought, particularly when downscaled and temporally extrapolated via data assimilation	Terrestrial Water Storage Mass Change Spatial Resolution: (450 km)^2 **Temporal Resolution: monthly** Accuracy: 25 mm	Terrestrial Water Storage Mass Change Spatial Resolution: (25 km)^2 **Temporal Resolution: weekly with <= weekly latency** Accuracy: 1.5 mm	**Baseline:** Consistency with the current program of record, which has supported quasi-operational groundwater and soil moisture drought monitoring with the aid of data assimilation. **Goal:** Enables drought monitoring at the spatial and temporal scales that water managers need without data assimilation. See Decadal Survey Table 6.4.
Earth Surface and Interior	***S-1.*** How can large-scale geological hazards be accurately forecast in a socially relevant timeframe?	S-1b. Measure and forecast interseismic, preseismic, coseismic, and postseismic activity over tectonically active areas on time scales ranging from hours to decades.	Land surface deformation Large scale gravity changes Reference Frame Topography Land cover change	Coseismic: +-1-2 uGal, Postseismic: >0.5 uGal/yr Spatial scale: (300 km)^2 (Han et al., 2019)	Most Important	High. MC provides a unique measurement for constraining long wavelength post-seismic processes	Post-seismic Relaxation **Spatial Resolution: (300km)^2** Temporal Resolution: monthly Accuracy: 1 uGal = 25 mm EWH	Post-seismic Relaxation: **Spatial resolution: (200 km)^2** Temporal Resolution: monthly Accuracy: 0.5 uGal = 12 mm EWH	**Baseline:** Consistency with the current program of record is needed for decadal scale postseismic and other seismic cycle processes. **Goal:** Improved spatial resolution and accuracy will enable better resolution of key seismic cycle processes and detection of M < 8.1 events
	S-3. How will local sea level change along coastlines around the world in the next decade to century?	S-3a. Quantify the rates of sea level change and its driving processes at global, regional, and local scales, with uncertainty < 0.1 mm yr-1 for global mean sea level equivalent and < 0.5 mm yr-1 sea level equivalent at resolution of 10 km.	Surface Melt Ice topography Snow density Mass Change 3-D surface deformation on ice Sea surface height Terrestrial Reference Frame In-situ temperature/salinity Ice velocity High resolution topography	Constraining GIA is important for estimating global sea level change and regionally for estimating ice mass change and assessing contribution to local sea level. GIA uncertainty varies spatially, peaking near 3.5 mm/yr relative sea level (Caron et al., 2018).	Most Important	High. MC is an essential component of global GIA estimates.	Glacial Isostatic Adjustment Spatial resolution: (300 km)^2 Temporal resolution: monthly **Accuracy: 25 mm**	Glacial Isostatic Adjustment Spatial resolution: (200 km)^2 Temporal resolution: monthly **Accuracy: 10 mm**	**Baseline:** Consistency with the current program of record is needed to estimate GIA and separate GIA from other signals. **Goal:** Specified in the Decadal Survey (Appendix B, gravity)
	S-4. What processes and interactions determine the rates of landscape change?	S-4a. Quantify global, decadal landscape change produced by abrupt events and by continuous reshaping of Earth's surface due to surface processes, tectonics, and societal activity.	Bare earth topography Land surface deformation Changes in optical surface characteristics Mass change Rain and snow fall rates Reflectance for freeze/thaw	See S-1b for abrupt changes in earthquakes	Most Important	Medium. Mass movement as discussed in other elements (earthquake related mass movement, ice mass change, and hydrological flux)	**Spatial Resolution: (300km)^2** Temporal Resolution: monthly Accuracy: 1 uGal = 25 mm EWH	**Spatial resolution: (200 km)^2** Temporal Resolution: monthly Accuracy: 0.5 uGal = 12 mm EWH	**Baseline:** Consistency with the current program of record is needed for abrupt to decadal scale seismic and other processes. **Goal:** Improved spatial resolution and accuracy will enable better resolution of key processes and detection of M < 8.1 events.
	S-5. How does energy flow from the core to the Earth's surface?	S-5a. Determine the effects of convection within the Earth's interior, specifically the dynamics of the Earth's core and its changing magnetic field and the interaction between mantle convection and plate motions. For MC: Determine exchange of angular momentum between core and mantle from changes in earth rotation parameters. To do this it is required to measure the xp and yp polar coordinates to a precision of 50 micro arcseconds. Source: Appendix B angular momentum variable, of Decadal Survey	Earth orientation parameters (VLBI) Mass change Reference frame Center of mass	Using existing mass change measurements, C_{21}, S_{21} are determined to ~2E-11 accuracy, which is 100x worse than needed to satisfy the targets listed in S-5a. (Wahr et al., 1987)	Very Important	Low. VLBI is the primary necessary observable	C_{21}/S_{21} only Spatial Resolution: (20,000 km)^2 Temporal Resolution: monthly **Accuracy: 2E-11 = 1 mm EWH**	C_{21}/S_{21} only Spatial Resolution: (20,000 km)^2 Temporal Resolution: monthly **Accuracy: 2E-13 = 0.01 mm EWH**	**Baseline:** Consistency with the current program of record. This is defined as the agreement between C_{21}/S_{21} derived from SLR and satellite gravimetry **Goal:** Improved accuracy of 2E-13 will allow for the determination of the angular offset between the Earth's figure axis and the mean mantle rotation axis to within 50 microarcseconds
	S-6. How much water is traveling deep underground and how does it affect geological processes and water supplies?	S-6b. Measure all significant fluxes in and out of the groundwater system across the recharge area	Soil moisture Snow water equivalent Rainfall Mass Change Topography Deformation from fluid fluxes Land surface deformation	See H-2c	Important	Medium. MC provides global long wavelength mass change.	Terrestrial Water Storage Mass Change **Spatial Resolution: (450 km)^2** Temporal Resolution: monthly Accuracy: 25 mm	Terrestrial Water Storage Mass Change **Spatial Resolution: (100 km)^2** Temporal Resolution: monthly Accuracy: 10 mm	**Baseline:** Consistency with the current program of record. **Goal:** Specified in the Decadal Survey (Appendix B, S-6b, gravity)

Table S1. Mass Change Science and Applications Traceability Matrix

Architecture	Summary
POD	24, 48, 96 satellites (absolute and relative baseline position data) Altitudes: 300 km Inclinations: Distributed evenly between 89° and 72°
SST single pair	2 satellites Altitudes: 350 km and 500 km Inclination: 89° Separation distances: 100, 300, 500 km
SST pendulum	2 satellites Altitudes: 350 km and 500 km Inclination: 89° Separation distances: 300 km Opening angle: 15 degrees and 45 degrees
SST pair + pendulum	3 satellites Altitudes: 350 km and 500 km Inclination: 89° Separation distances: 300 km Opening angle: 15 degrees and 45 degrees
SST dual pair (Bender)	4 satellites Altitudes: 350 km and 500 km Altitude combinations: high/high; high/low; low/high; low/low Inclinations: 89° and 72° Separation distances: 100, 300, 500 km
LEO-MEO 1	4/5/7 satellites LEO altitude: 350 km and 500 km MEO altitude: 7000 km Inclination: 89° and 72° Combinations: 1 LEO + 3 MEO; LEO SST pair + 3 MEO; LEO SST dual pair + 3 MEO
LEO-MEO 2	8 satellites LEO altitude: 500 km MEO altitude: 1500 km Inclination: 89° Combinations: LEO SST pair + 6 MEO
AIGG	1 satellite (radial pointing) Altitudes: 350 km and 500 km

Table S2. Summary of simulated architectures

Satellite-to-Satellite Ranging Technology	Performance vs. GRACE-FO LRI	Size Weight and Power vs. LRI	Current Technology Readiness Level[†]
GRACE-FO MWI	0.01×	1×	9
GRACE-FO LRI	1×	1×	9
Ball optical frequency comb	1× (allows for pendulum)	1×	5
GeoOptics K-/V-band ranging	0.01×	0.1× (SW) 0.5× (P)	6
GSFC μNPRO	0.5×	0.4× (SW) 0.6× (P)	5
LMI transponder (ESA)	1×	1×	4
LMI retroreflector (ESA)	1× (limited to smaller distances)	1×	4
Laser chronometer (CNES)	0.01× (gimbaled for pendulum)	0.5× (SW) 1.5× (P)	4

[†] Vendor-assessed TRL of lowest element level component at completion of the study

Table S3. Summary of satellite-to-satellite ranging technologies. Performance numbers are approximations and represent relative performance at approximately 10 mHz. The

"X" in the table indicates "times"; for instance, the GRACE-FO MWI performance is 0.01 times the performance of the GRACE-FO LRI

Accelerometer Technology	**Performance vs. GRACE-FO**	**Size Weight and Power vs. GRACE-FO**	**Current TRL**[†]
ONERA GRACE-FO electrostatic	1✕	1✕	9
ONERA MicroSTAR-Prime electrostatic	1.7✕ with 3-axis sensitivity	1✕	4
ONERA MicroSTAR electrostatic	30✕ with drag compensation	1✕	4
ONERA HybridSTAR ES + cold atom	60✕ with drag compensation	10✕	3
Simplified LISA Pathfinder Gravitational Reference Sensor (S-GRS)	20✕ without drag compensation 200✕ with drag compensation	1✕	2
ONERA CubSTAR electrostatic	1✕	0.3✕	3
Compact optomechanical inertial sensor	0.05✕ – 0.4✕	0.01✕	2

[†] Vendor-assessed TRL of lowest element level component at completion of the study

Table S4. Summary of accelerometer technologies. Performance numbers are approximations and represent relative performance at approximately 1 mHz. The "X" in the table indicates “times”; for instance, the S-GRS performance with drag compensation is 200 times the performance of the GRACE-FO accelerometer.

	Truth Model	**Nominal Model**
Static Gravity Field	gif48	gif48
Ocean Tides	GOT4.8	FES2004
Nontidal Atmosphere and Ocean (AOD)	AOD RL05	AOerr + DEAL (Dobslaw et al., 2016)
Hydrology + Ice	ESA Earth System Model	

Table S5. Force models used in numerical simulations